

# Goos-Hänchen and Imbert-Fedorov shifts for Gaussian beams impinging on graphene-coated surfaces

Simon Grosche, Marco Ornigotti and Alexander Szameit

*Institute of Applied Physics, Friedrich-Schiller-Universität Jena,  
Max-Wien-Platz 1, D-07743 Jena, Germany*

Compiled November 10, 2021

We present a theoretical study of the Goos-Hänchen and Imbert-Fedorov shifts for a fundamental Gaussian beam impinging on a surface coated with a single layer of graphene. We show that the graphene surface conductivity  $\sigma(\omega)$  is responsible for the appearance of a giant and negative spatial Goos-Hänchen shift. © 2021 Optical Society of America

OCIS codes: 240.3695, 260.2110,

When an optical beam impinges upon a surface, non-specular reflection phenomena may occur, such as the Goos-Hänchen (GH) [1–3] and Imbert-Fedorov (IF) [4,5] shifts, resulting in an effective beam shift at the interface. A comprehensive review on beam shift phenomena can be found in Ref. [6]. Although Goos and Hänchen published their work more than 60 years ago [1], this field of research is still very active, and in the last decades a vast amount of literature has been produced on the subject, resulting not only in a better understanding of the underlying physical principles [7–14], but also in the careful investigation of the effects of various field configurations [?, 15, 17–19] and reflecting surfaces [20–23] on the GH and IF shifts.

In recent years, on a parallel trail, graphene attracted very rapidly a lot of interest, thanks to its intriguing properties [24, 25]. Its peculiar band structure and the existence of the so-called Dirac cones [26], for example, give the possibility to use graphene as a model to observe QED-like effects such as Klein tunneling [27], Zitterbewegung [28], the anomalous quantum Hall effect [29] and the appearance of a minimal conductivity that approaches the quantum limit  $e^2/h$  for vanishing charge density [30]. In addition, the reflectance and transmittance of graphene are determined by the fine structure constant [31], and a single layer of graphene shows universal absorbance in the spectral range from near-infrared to the visible part of the spectrum [32].

Among the vast plethora of applications, graphene also proved to be a very interesting system where to observe beam shifts. Very recently, in fact, the occurrence of GH shift in graphene-based structures has been reported, both for light beams (where giant GH shift has been observed [33]) and for Dirac fermions [34]. Despite all this, a full theoretical analysis of GH and IF shifts in a graphene-based structure has not been yet carried out.

In this Letter, we therefore present a theoretical analysis of the GH and IF shifts occurring for a monochromatic Gaussian beam impinging onto a glass surface coated with a single layer of graphene. The results of our investigations show on one hand, that the appearance of

a giant GH shift is ultimately due to the graphene’s surface conductivity  $\sigma(\omega)$ , and on the other hand, that the presence of the single layer of graphene introduces a dependence of the phases of the reflection coefficients on the incidence angle, thus resulting in a nonzero spatial GH shift also when total internal reflection does not occur.

We start our analysis by considering a monochromatic Gaussian beam with frequency  $\omega = ck$  (with  $k$  being the vacuum wave number), impinging on a dielectric surface characterized by the refractive index  $n$  and coated with a single layer of graphene [Fig. 1 (a)]. The graphene layer is characterized by the optical conductivity  $\sigma(\omega)$ , whose expression can be given in the following dimensionless form [26]

$$\sigma(\Omega) = i \frac{4\alpha}{\Omega} + \pi\alpha \left[ \Theta(\Omega - 2) + \frac{i}{2\pi} \ln \frac{(\Omega - 2)^2}{(\Omega + 2)^2} \right], \quad (1)$$

where  $\Omega = \hbar\omega/\mu$  is the dimensionless frequency,  $\mu$  is the chemical potential,  $\alpha \approx 1/137$  is the fine structure constant [28] and  $\Theta(x)$  is the Heaviside step function [35].

According to Fig. 1(b), we define three Cartesian reference frames: the laboratory frame  $K = (O, x, y, z)$  attached to the reflecting surface, the (local) incident frame  $K_i = (O, x_i, y, z_i)$  attached to the incident beam, and the (local) reflected frame  $K_r = (O, x_r, y, z_r)$  attached to the reflected beam. These three reference frames are connected via a rotation of an angle  $\theta$  around the  $y$  direction [37]. The reflecting surface is located at  $z = 0$ , with the  $z$ -axis pointing towards the interface. With this choice of geometry, the incident beam comes from the region  $z < 0$  and propagates in the  $x$ - $z$  plane.

The electric field in the incident frame can be then written, using its angular spectrum representation [36], as follows:

$$\mathbf{E}_i(\mathbf{r}) = \sum_{\lambda=1}^2 \int d^2K \hat{\mathbf{e}}_\lambda(U, V, \theta) A_\lambda(U, V, \theta) e^{i\mathbf{k}_i \cdot \mathbf{r}_i}, \quad (2)$$

where  $d^2K = dUdV$ ,  $\hat{\mathbf{e}}_\lambda(U, V, \theta)$  is the local reference frame attached to the incident field [38],  $A_\lambda(U, V, \theta) =$

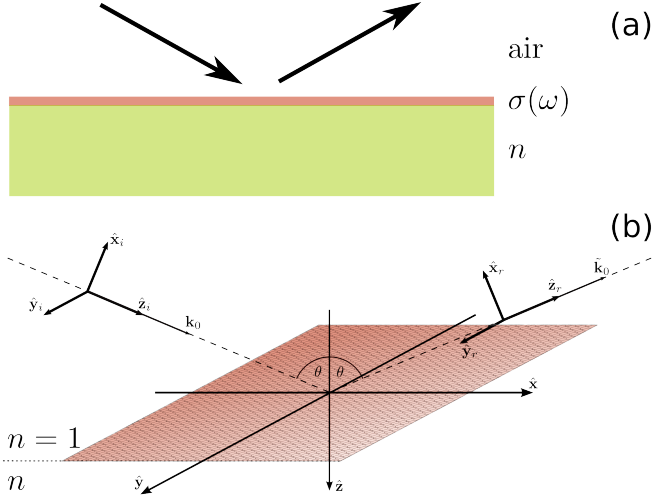


Fig. 1. (Color online) (a) Schematic representation of the considered surface. The graphene layer (red) is characterized by its surface conductivity  $\sigma(\Omega)$ , whose explicit expression is given by Eq. (1). The dielectric substrate (green) is characterized by the refractive index  $n$ . (b) Geometry of beam reflection at the interface. The single graphene layer is located on the surface at  $z = 0$ . The different Cartesian coordinate systems  $K, K_i, K_r$  are shown.

$\alpha_\lambda(U, V, \theta)A(U, V)$  and  $\mathbf{k}_i \cdot \mathbf{r}_i = UX_i + VY_i + WZ_i$ , being  $X_i = k_0 x_i$  the normalized coordinate in the incident frame.  $Y_i$  and  $Z_i$  are defined in a similar manner.  $\alpha_\lambda(U, V, \theta) = \hat{\mathbf{e}}_\lambda(U, V, \theta) \cdot \hat{\mathbf{f}}$  accounts for the projection of the beam's polarization  $\hat{\mathbf{f}} = f_p \hat{\mathbf{x}} + f_s \hat{\mathbf{y}}$  (normalized according to  $|f_p|^2 + |f_s|^2 = 1$ ) onto the local basis, and  $A(U, V)$  is the beam's spectral amplitude, which here is assumed to be Gaussian, i.e.,

$$A(U, V) = e^{-w_0^2(U^2+V^2)}, \quad (3)$$

being  $w_0^2$  the spot size of the beam. In the remaining of the manuscript, we will consider only well collimated beams, namely the paraxial assumption  $U, V \ll 1$  is implicitly understood.

Upon reflection, the electric field can be then written as follows:

$$\mathbf{E}_r(\mathbf{r}_r) = \sum_{\lambda=1}^2 \int d^2K \hat{\mathbf{e}}_\lambda(-U, V, \pi - \theta) \tilde{A}_\lambda(U, V, \theta) e^{i\mathbf{k}_r \cdot \mathbf{r}_r}, \quad (4)$$

where  $\mathbf{k}_r \cdot \mathbf{r}_r = -UX_r + VY_r + WZ_r$  and  $\tilde{A}_\lambda(U, V, \theta) = r_\lambda(U, V, \theta)A_\lambda(U, V, \theta)$ , with  $r_\lambda(U, V, \theta)$  being the Fresnel reflection coefficients associated to the single plane wave component of the field [39]. The minus sign in front of  $U$  in  $\hat{\mathbf{e}}_\lambda$ , as well as in  $\mathbf{k}_r \cdot \mathbf{r}_r$  accounts for the specular reflection of the single plane wave component [38].

The presence of a single layer of graphene deposited on the dielectric surface modifies its reflection coefficients as

follows [40]:

$$r_s(\theta) = \frac{\cos \theta - \sqrt{n^2 - \sin^2 \theta} - \sigma(\Omega)}{\cos \theta + \sqrt{n^2 - \sin^2 \theta} + \sigma(\Omega)}, \quad (5a)$$

$$r_p(\theta) = \frac{n^2 \cos \theta - \sqrt{n^2 - \sin^2 \theta} [1 - \sigma(\Omega) \cos \theta]}{n^2 \cos \theta + \sqrt{n^2 - \sin^2 \theta} [1 + \sigma(\Omega) \cos \theta]}, \quad (5b)$$

where  $\theta$  is the incident angle,  $n$  is the refractive index of the dielectric medium and  $\sigma(\Omega)$  is the graphene's surface conductivity, as defined by Eq. (1). The modulus  $R_\lambda$  and phase  $\phi_\lambda$  of the reflection coefficients  $r_\lambda = R_\lambda e^{i\phi_\lambda}$  (with  $\lambda \in \{p, s\}$ ) are shown in Fig. 2, together with the correspondent quantities for the case of a simple dielectric surface without the graphene coating. While the presence of the graphene layer does not modify significantly  $R_\lambda$  for neither  $p$ - or  $s$ -polarization (as it appears clear from Figs. 2(a) and (c), respectively), the change induced in the phases  $\phi_\lambda$  of the reflection coefficients is considerable. For a normal air-glass interface, in fact, we have  $\partial\phi_\lambda/\partial\theta = 0$  being  $\theta$  the angle of incidence. Here, instead, we have  $\partial\phi_\lambda/\partial\theta \neq 0$ . A closer inspection of Eqs. (5), moreover, reveals that such a novel  $\theta$ -dependence of the phases  $\phi_\lambda$  is entirely due to the graphene conductivity  $\sigma(\Omega)$ .

To compute the GH and IF shifts, we calculate the center of mass of the intensity distribution in the reflected frame, namely [38]

$$\langle \mathbf{R} \rangle = \frac{\iint_{-\infty}^{+\infty} \mathbf{R} |\mathbf{E}_r|^2 dX_r dY_r}{\iint_{-\infty}^{+\infty} |\mathbf{E}_r|^2 dX_r dY_r} = \langle X_r \rangle \hat{\mathbf{X}}_r + \langle Y_r \rangle \hat{\mathbf{Y}}_r, \quad (6)$$

where  $\mathbf{R} = (X_r, Y_r)^T$ . Spatial ( $\Delta$ ) and angular ( $\Theta$ ) GH and IF shifts are then defined as follows:

$$\Delta_{GH} = \langle X_r \rangle \Big|_{z=0}, \quad \Theta_{GH} = \frac{\partial \langle X_r \rangle}{\partial z}, \quad (7a)$$

$$\Delta_{IF} = \langle Y_r \rangle \Big|_{z=0}, \quad \Theta_{IF} = \frac{\partial \langle Y_r \rangle}{\partial z}. \quad (7b)$$

The explicit expressions of the GH and IF shifts for a fundamental Gaussian beam read, according to [41], as follows:

$$\Delta_{GH} = w_p \frac{\partial \phi_p}{\partial \theta} + w_s \frac{\partial \phi_s}{\partial \theta}, \quad (8a)$$

$$\Delta_{IF} = -\cot \theta \left[ \frac{w_p a_s^2 + w_s a_p^2}{a_p a_s} \sin \eta + 2\sqrt{w_p w_s} \sin(\eta - \phi_p + \phi_s) \right], \quad (8b)$$

$$\Theta_{GH} = - \left( w_p \frac{\partial \ln R_p}{\partial \theta} + w_s \frac{\partial \ln R_s}{\partial \theta} \right), \quad (8c)$$

$$\Theta_{IF} = \frac{w_p a_s^2 - w_s a_p^2}{a_p a_s} \cos \eta \cot \theta, \quad (8d)$$

where  $f_p = a_p$ ,  $f_s = a_s \exp(i\eta)$  and  $w_\lambda = a_\lambda^2 R_\lambda^2 / (a_p^2 R_p^2 + a_s^2 R_s^2)$  (where  $\lambda \in \{p, s\}$ ) is the fractional energy contained in each polarization state.

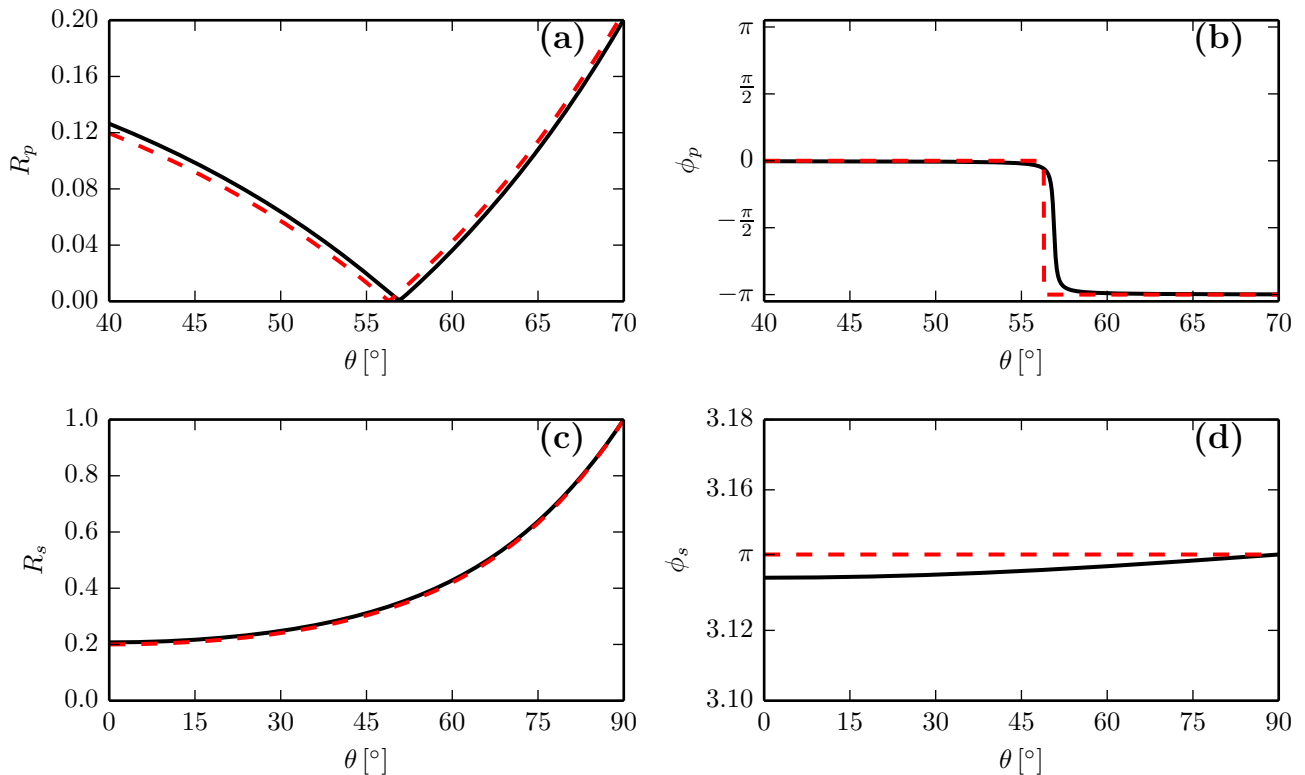


Fig. 2. Modulus (left column) and phase (right column) of the reflection coefficients  $r_\lambda = R_\lambda \exp(i\phi_\lambda)$  for  $p$ -polarization (top row) and  $s$ -polarization (bottom row). In all graphs, the solid black line corresponds to the case of the graphene-coated surface, while the red dashed curve corresponds to the case without graphene coating. The refractive index of the bulk medium is chosen to be  $n = 1.5$ .

As suggested by Figs. 2(a) and (c), the changes in  $R_\lambda$  introduced by the graphene layer are negligible. We therefore expect to observe no changes in the angular shifts  $\Theta_{GH}$  and  $\Theta_{IF}$ , as they are functions of  $R_\lambda$  solely. The spatial shifts  $\Delta_{GH}$  and  $\Delta_{IF}$ , on the other hand, contain a dependence on the phases  $\phi_\lambda$ , and they are therefore affected by the presence of the graphene coating. Let us first discuss the IF shift. In this case  $\phi_p - \phi_s$  is very close to  $\pi$  [Figs. 2(b) and (d)], and the resulting spatial shift  $\Delta_{IF}$  will be *nonzero* (but very small) even for linear polarization, in contrast to the case without graphene.

More interesting is the case of the spatial GH shift. For a normal air-dielectric interface, one has  $\partial\phi_\lambda/\partial\theta = 0$  and therefore, according to Eq. (8a),  $\Delta_{GH} = 0$ . It is in fact well known since the pioneering work of Goos and Hänchen [1], that  $\Delta_{GH} \neq 0$  occurs only in total internal reflection, where  $R_\lambda = 1$  and  $\partial\phi_\lambda/\partial\theta \neq 0$ . For the case of a graphene-coated surface, on the other hand, the phase  $\phi_\lambda$  varies with  $\theta$  for both  $s$ - and  $p$ -polarizations, as Figs. 2 (b) and (d), respectively, show. In this case, then, we observe a *nonzero* spatial GH shift even without total internal reflection.

The spatial GH shift  $\Delta_{GH}$  occurring at a graphene-

coated dielectric surface is depicted in Fig. 3(a) and (b) for  $p$ - and  $s$ -polarization, respectively. As can be seen, for both polarizations we have  $\Delta_{GH} \neq 0$  although no total internal reflection takes place. In particular,  $\phi_p$  varies very rapidly from 0 to  $-\pi$  in the vicinity of the Brewster angle  $\theta_B$ . This corresponds to a giant and negative spatial GH shift. On the other hand,  $\phi_s$  varies very smoothly with  $\theta$ , thus resulting in a *nonzero* (but very small) spatial GH shift for  $s$ -polarization.

In conclusion, we have presented a detailed theoretical analysis of GH and IF shifts of a Gaussian beam impinging onto a graphene-coated dielectric surface. Our analysis revealed that the main effect of the graphene layer is to introduce, through its surface conductivity  $\sigma(\omega)$ , a dependence of the phases  $\phi_\lambda$  of the reflection coefficients on the incident angle  $\theta$ . This, ultimately, reflects in the appearance of a *nonzero* spatial GH and IF shifts. In particular a giant and negative spatial GH shift in the vicinity of the Brewster's angle for  $p$ -polarization has been predicted, in agreement with the recently published experimental results [33]. The authors thank the German Ministry of Education and Science (ZIK 03Z1HN31) for financial support.

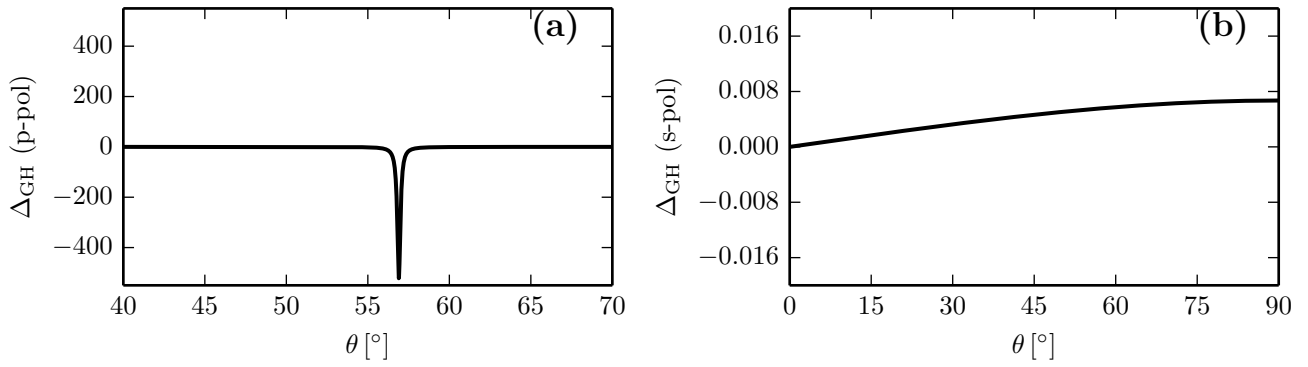


Fig. 3. Spatial GH shift  $\Delta_{GH}$  for (a)  $p$ - polarization and (b)  $s$ -polarization for a graphene-coated surface. Since  $\partial\phi_\lambda/\partial\theta \neq 0$ , in both cases  $\Delta_{GH} \neq 0$ . In particular, since  $\phi_p$  varies very rapidly with  $\theta$  in the vicinity of the Brewster angle, the corresponding spatial shift for  $p$ -polarization [Panel (a)] is giant in modulus, and negative due to the fact that  $\phi_p$  varies from 0 to  $-\pi$  [See Fig. 2(b)].

## References

1. F. Goos and H. Hänchen, *Ann. Phys.* **1**, 333 (1947).
2. K. Artmann, *Ann. Phys.* **2**, 87 (1948).
3. K. W. Chiu and J. J. Quinn, *Am. J. Phys.* **40**, 1847 (1972)
4. F. I. Fedorov, *Dokl. Akad. Nauk SSSR* **105**, 465 (1955).
5. C. Imbert, *Phys. Rev. D* **5**, 787 (1972).
6. K. Y. Bliokh and A. Aiello, *J. Opt.* **15**, 014001 (2013).
7. F. Pillon, H. Gilles and S. Girard, *Appl. Opt.* **43**, 1863 (2004).
8. H. Schilling, *Ann. Phys. (Berlin)* **16**, 122 (1965).
9. M. A. Player, *J. Phys. A: Math. Gen.* **20**, 3667 (1987).
10. V. G. Fedoseyev, *J. Phys. A: Math. Gen* **21**, 2045 (1988).
11. V. S. Liberman and B. Y. Zel'dovich, *Phys. Rev. A* **46**, 5199 (1992).
12. K. Y. Bliokh and Y. P. Bliokh, *Phys. Rev. Lett.* **96**, 073903 (2006).
13. A. Aiello and J. P. Woerdman, *Opt. Lett.* **33**, 1437 (2008).
14. O. Hosten and P. Kwiat, *Science* **319**, 787 (2008).
15. P.T. Leung, C. W. Chen and H. -P. Chiang, *Opt. Commun.* **276**, 206 (2007).
16. M. Merano, A. Aiello, G. W. 't Hooft, M. P. von Exter, E. R. Eliel and J. P. Woerdman, *Opt. Expr.* **15**, 15928 (2007).
17. T. Tamir, *J. Opt. Soc. Am. A* **3**, 558 (1986).
18. G. D. Landry and T. A. Maldonado, *Appl. Opt.* **35**, 5870 (1996).
19. M. Ornigotti, A. Aiello and C. Conti, *Opt. Lett.* **40**, 558 (2015).
20. S. Kozaki and H. Sakurai, *J. Opt. Soc. Am.* **68**, 508 (1978).
21. D. Golla and S. Dutta Gupta, arXiv:1011.3968v1.
22. M. Merano, N. Hermosa, J.P. Woerdman and A. Aiello, *Phys. Rev. A* **82**, 023817 (2010).
23. A. Aiello and J. P. Woerdman, *Opt. Lett.* **36**, 543 (2010).
24. K. S. Novoselov, A. K. Geim, S. V. Morozov, D. Jiang, M. I. Katsnelson, I. V. Grigorieva, S. V. Dubonos and A. A. Firsov, *Nature* **438**, 197 (2005).
25. A. H. Castro Neto, F. Guinea, N. M. R. Peres, K. S. Novoselov, and A. K. Geim, *Rev. Mod. Phys.* **81**, 109 (2009).
26. M. I. Katsnelson, *Graphene: Carbon in Two Dimensions* (Cambridge University Press, 2012).
27. A. Calogeracos, N. Dombey, *Contemp. Phys.* **40**, 313 (1999).
28. C. Itzykson and J. B. Zuber, *Quantum Field Theory* (Dover, 2006).
29. Y. Zhang, Y. W. Tan, H. L. Stormer and P. Kim, *Nature* **438**, 201 (2005).
30. M. I. Katsnelson, *Eur. Phys. J. B.* **51**, 157 (2006).
31. R. R. Nair, P. Blake, A. N. Grigorenko, K. S. Novoselov, T. J. Booth, T. Stauber, N. M. R. Peres and A. K. Geim, *Science* **320**, 1308 (2008).
32. T. Stauber, N. M. R. Peres, and A. K. Geim, *Phys. Rev. B* **78**, 085432 (2008).
33. X. Li, P. Wang, F. Xing, X. D. Chen, Z. B. Liu, and J. G. Tian, *Opt. Lett.* **39**, 5574 (2014).
34. A. Jellala, I. Redouanic, Y. Zahidic and H. Bahloulia, *Physica E* **58**, 30 (2014).
35. *Digital Library of Mathematical Functions*, <http://dlmf.nist.gov>, National Institute of Standard and Technology (2010).
36. L. Mandel and E. Wolf, *Optical Coherence and Quantum Optics*, (Cambridge University Press, New York, 1995).
37. M. Merano A. Aiello and J. P. Woerdman, *Phys. Rev. A* **80**, 061801(R) (2009).
38. A. Aiello and J. P. Woerdman, arXiv:0903.3730v2 [physics.optics].
39. M. Born and E. Wolf, *Principles of Optics*, 7th edition (Cambridge University Press, 2003).
40. T. Zhan, X. Shi, Y. Dai, X. Liu and J. Zi, *J. Phys.: Condens. Matt.* **25**, 215301 (2013).
41. M. Ornigotti and A. Aiello, *J. Opt.* **15**, 014004 (2013).